

Rapid Communications

The Rapid Communications section is intended for the accelerated publication of important new results. Manuscripts submitted to this section are given priority in handling in the editorial office and in production. A Rapid Communication may be no longer than 3½ printed pages and must be accompanied by an abstract. Page proofs are sent to authors, but, because of the rapid publication schedule, publication is not delayed for receipt of corrections unless requested by the author.

Direct measurement of the velocity dependence of the associative-ionization cross section in $\text{Na}(3p) + \text{Na}(3p)$ collisions

M-X. Wang, M. S. de Vries, J. Keller, and J. Weiner

Department of Chemistry, University of Maryland, College Park, Maryland 20742

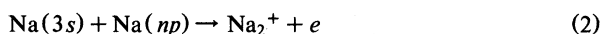
(Received 2 April 1985)

We present a direct measurement of the velocity dependence of the associative-ionization (AI) cross section for collisions between $\text{Na}(^3P)$ atoms in the energy range 0.08–0.29 eV in a crossed-beam experiment using a Doppler-shift velocity selection technique. The AI cross section at first decreases, reaches a minimum at about 0.15 eV, then sharply increases with collision energy. Interpretation of the results in terms of a semiclassical theory of AI indicates that more than one potential surface of $\text{Na}(^2P + ^2P)$ must be involved in the AI process.

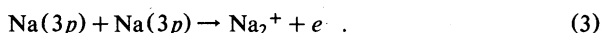
In recent years, laser-assisted associative ionization (AI) between optically excited alkali atoms has become an intriguing research field both to theorists and experimentalists. The reaction is of the general form



where A^* represents atoms in excited states. For the case of sodium, absolute rate-constant measurements have been reported for the series of reactions¹



and for the AI reaction between two resonantly excited atoms^{2,3}



Surprisingly, the results show that the rate constant for (3) is almost two orders of magnitude smaller than those for (2). Other studies of (3) (Refs. 4–6) suggest that the AI probability may strongly correlate with collision velocity; and indeed, as can be seen from Fig. 1, the relative energy position of the Na_2^+ potential minimum with respect to the molecular potential curves deriving from $\text{Na}(3p) + \text{Na}(3p)$ lends credence to this possibility. If the AI collision dynamic follows one or more repulsive curves, then the system presents a barrier to the reaction; and one would expect a low velocity-averaged cross section (rate constant) but a reaction probability rising rapidly with collision velocity.

The experiment reported here measures directly the velocity dependence of AI cross section in $\text{Na}(3p) + \text{Na}(3p)$ collisions. We achieve highly resolved velocity selection through laser excitation of narrow velocity groups in the Doppler profile of two crossed Na beams. By offsetting the excitation laser frequency from the resonance atomic frequency ν_0 for a stationary atom, the Doppler shift exactly compensates for the laser detuning and brings the group of atoms with velocity $v = \lambda_0(\nu - \nu_0)$ back into resonance.

Although the idea of using Doppler spectroscopy in cell experiments was developed about a decade ago by Pritchard and co-workers,^{7,8} the inherent advantages of the technique are significantly enhanced in the present crossed-beams experiment for two reasons: (1) For the special case of $\text{Na}^*(3p) + \text{Na}^*(3p)$ AI, both collision partners are optically excited so both beams are velocity selected; (2) the crossed-beam configuration can achieve a wider range of high-resolution velocity selection by greatly reducing velocity components transverse to the excitation axis. It is also a single collision environment which eliminates the possibility of secondary processes such as superelastically heated electron-atom excitation or ionization.

Figure 2 shows a schematic of the apparatus in the hor-

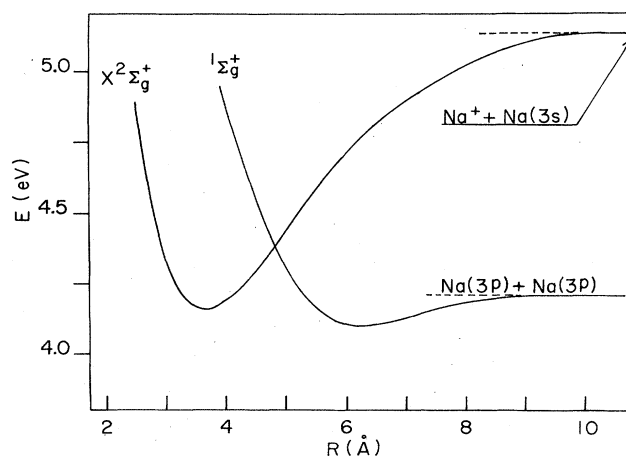


FIG. 1. Ground-state potential curve of Na_2^+ and one recently calculated excited-state curve arising from the $\text{Na}^*(3p) + \text{Na}^*(3p)$ asymptotic level.

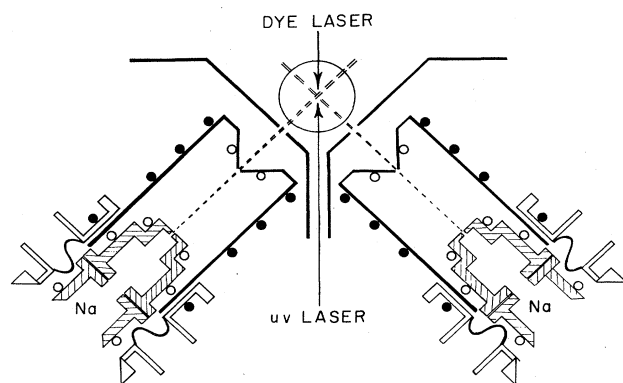


FIG. 2. Schematic diagram of the apparatus. Open circles indicate heating elements; closed circles are cooling elements.

horizontal plane containing two atomic-beam sources oriented at 90° . A high-resolution cw ring dye laser (Coherent CR-699, 0.1 W, bandwidth=1 MHz) excites sodium atoms to $3p^2P_{3/2}$ ($F=3$) state. A uv laser (argon ion, 0.3 W, $\lambda=351$ nm) collinear with and counterpropagating to the dye-laser probes the excited atomic state population by selective photoionization out of the $3p$ level. The two lasers bisect the angle between the sodium beams. In order to take full advantage of the dye-laser spectral resolution, we employ two collimated atomic beams with angular divergence of no more than 35 mrad. A liquid-nitrogen-cooled baffle placed downstream from the beam orifice and around the interaction region keeps the collision zone free from background interference. A nested pair of kinematic planes upon which the source and skimmer are mounted gives us convenient control of source-skimmer alignment and relative beam-beam orientation. Finally, the atomic-beam sources are fitted to ports on a high-vacuum cylindrical chamber surrounded by a liquid-nitrogen reservoir. The oven operating temperature is 500°C , producing an intensity of $5.2 \times 10^{10} \text{ cm}^{-3}$ in the interaction region. As determined by Fischer and Hertel,⁹ this is just below the density at which radiation trapping becomes significant. The Na_2^+ ions produced in the collision region are accelerated upward (field intensity=10 V/cm) and collected by a Cu-Be focused mesh particle multiplier (Johnston Laboratories MM-1). The signal current is then fed to a discriminator-amplifier and recorded on a X-Y plotter as a function of dye-laser frequency. We calibrate the absolute frequency of the ring dye laser with iodine cell absorption spectrum and the frequency scan interval with a Fabry-Perot interferometer. In order to suppress optical pumping effects, we impose an axis of quantization with a magnetic field of several gauss collinear with the laser beam propagation axis. The dye laser is circularly polarized in order to confine the transition to the $M_F=2$ and $M_F=3$ Zeeman components of the lower $^2S_{1/2}$ and $^2P_{3/2}$ upper states, respectively.

The AI rate equation is

$$\frac{d[\text{Na}_2^+]}{dt} = \sigma_{\text{AI}} v [\text{Na}(3p)]^2, \quad (4)$$

where σ_{AI} is the AI cross section and v is the relative velocity between two atomic beams. The bracketed quantities represent number densities.

The rate equation for $\text{Na}(3p)$ photoionization is given by

$$\frac{d[\text{Na}^+]}{dt} = \Phi_{\text{ph}} \sigma_{\text{ph}} [\text{Na}(3p)], \quad (5)$$

where σ_{ph} is the photoionization cross section and Φ_{ph} the photon flux of the photoionizing laser.

Combining (4) and (5), we have

$$\sigma_{\text{AI}} = \frac{I(\text{Na}_2^+)}{I(\text{Na}^+)^2} \frac{(\Phi_{\text{ph}} \sigma_{\text{ph}})^2}{v}, \quad (6)$$

where $I(\text{Na}_2^+) = d[\text{Na}_2^+]/dt$ and $I(\text{Na}^+) = d[\text{Na}^+]/dt$. The relative velocity v is determined from direct measure of the laboratory velocity distribution in each beam (see Fig. 2). Therefore, by measuring the ratio of $I(\text{Na}_2^+)$ to $I(\text{Na}^+)$ as a function of dye-laser frequency, we obtain the AI cross section as a function of collision velocity.

We consecutively measure $I(\text{Na}_2^+)$ and $I(\text{Na}^+)$ by scanning the dye laser over the velocity distribution while alternately blocking and unblocking the uv laser. With the uv laser blocked the signal is due entirely to AI, and with it unblocked the total signal is due to the sum of AI and photoionization of $\text{Na}^*(3p)$. The photoionization signal is 10 times larger than the collisional ionization signal which therefore makes a negligible contribution to the unblocked profile. In the center of the collision chamber, a bright fluorescence dot (0.25 cm^3) shows clearly where the laser intersects the crossing region of the two atomic beams. Horizontally displacing the dye-laser beam away from the collision center results in complete disappearance of Na_2^+ signal, demonstrating that ionization is indeed produced by an interbeam collisional process. We further confirm the ion identity by time-of-flight mass analysis which shows that Na_2^+ is the only ion species produced in the collision reaction.

Figure 3 shows the atomic velocity distribution in a single beam. The curve is narrower and shifted towards a higher velocity than a Maxwell-Boltzmann distribution at the same temperature. The measured velocity profile fits quite well the distribution of a Mach 6 free jet expansion.¹⁰

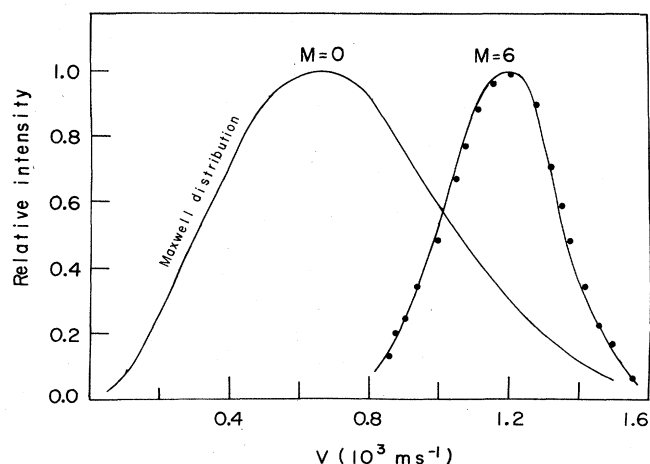


FIG. 3. Closed circles are the measured speed distribution of one Na jet. Note excellent fit to distribution calculated from a Mach 6 supersonic jet at 500°C .

Experimental results are plotted in Fig. 4. The AI cross section at first decreases, reaches a minimum, then sharply increases with collision energy. The horizontal error bars are determined essentially by Na beam divergence while the vertical error bars are calculated from atomic-beam divergence and signal fluctuation in Na^+ and Na_2^+ .

We have carried out a model calculation of the AI cross section as a function of collision energy using the semiclassical treatment of Miller.¹¹ Since Penning ionization is not energetically possible in $\text{Na}(3p) + \text{Na}(3p)$ collision ionization, the probability for AI is given by

$$P(E, b) = 1 - \exp\left[-2 \int_{R_0}^{\infty} \frac{\Gamma(R)}{\hbar v} dR\right], \quad (7)$$

where E, b are the total energy and impact parameter, R_0 the classical turning point on the $\text{Na}(^2P + ^2P)$ potential $V^*(R)$, $\Gamma(R)$ the resonance width, and v the radial velocity calculated from

$$v = \left\{ \frac{2}{\mu} \left[E \left(1 - \frac{b^2}{R^2} \right) - V^*(R) \right] \right\}^{1/2}, \quad (8)$$

where μ is the reduced mass. The cross section of AI is then given by

$$\sigma(E) = 2\pi \int_0^{\infty} P(E, b) b db. \quad (9)$$

While the $X^2\Sigma_g^+$ ground state of Na_2^+ is well known,¹² the only excited-state potential curve available for $\text{Na}(^2P + ^2P)$ is the one calculated by Montagnani, Riani, and Salvetti,¹³ which crosses the $X^2\Sigma_g^+$ state of Na_2^+ at collision energies of about 0.19 eV. We have fitted the theoretical calculation with the measured cross section, assuming for the resonant width the exponential form

$$\Gamma(R) = Ae^{-sR} \quad (10)$$

and adjusting the s and A parameters. The best fit has been obtained for $s = 3.3 \text{ \AA}^{-1}$, $A = 500 \text{ eV}$ in the collision energy range between 0.19 and 0.29 eV (corresponding to the region where the cross section increases with energy). With this choice of s and A values and using Eqs. (7)–(10), we estimate the absolute AI cross section to be from 2 to 8 \AA^2 in this energy region. The calculation indicates that the $X^1\Sigma_g^+$ state of $\text{Na}(^2P + ^2P)$ participates in the process; but since it cannot account for the low-energy part (below 0.19 eV) of the AI cross-section curve, there must be at least another potential surface of $\text{Na}(^2P + ^2P)$ involved. Combining the recent alignment experiments^{14,15} with Doppler velocity selection would increase the specificity of the state selection even further.

The present experiment is carried out in a higher collision energy range (0.08–0.29 eV) than the previously reported absolute measurements (0.005–0.08 eV) of AI rate coeffi-

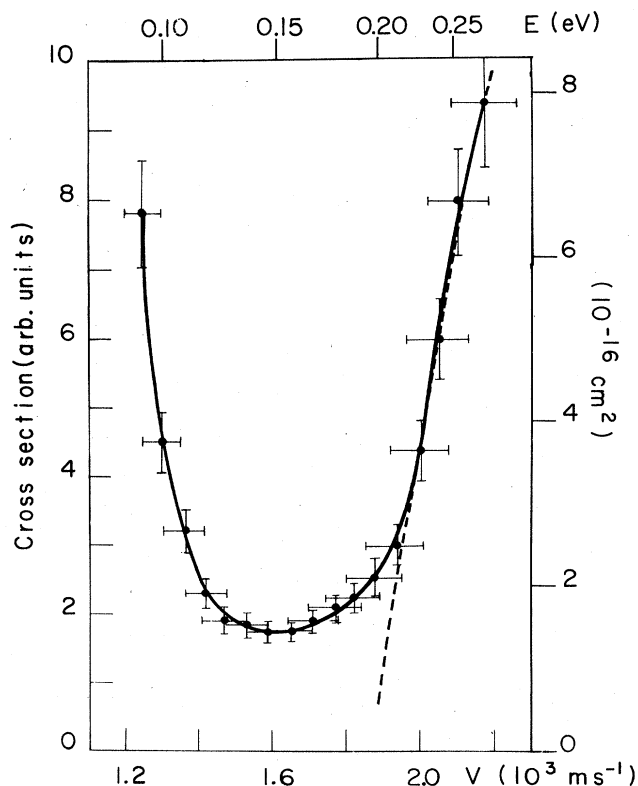


FIG. 4. Cross section from AI vs relative energy (upper abscissa) and relative velocity (lower abscissa). Dashed line is fit using Eqs. (7)–(10) of text and the excited-state potential of Fig. 1. The steeply descending portion of the curve at lower velocity may be due to another, more attractive potential.

icients.^{2–6} Measurement of the AI cross section as a function of collision velocity in this lower energy range is necessary in order not only to compare the results of these two types of measurements, but also to reveal any possible resonance features in the collision energy spectrum.¹⁶ It is hoped that the present study will stimulate more theoretical efforts¹⁷ to calculate the relevant potential curves of $\text{Na}(^2P + ^2P)$ which are essential to improve our understanding of the associative-ionization process.

We wish to express our appreciation to the Regional Laser Laboratory of the University of Pennsylvania and especially Dr. Gary Holtom for providing the ring dye laser and other generous help in the course of the experiment. This work was supported in part by National Science Foundation Grant No. PHY-83-05086.

¹J. Boulmer, R. Bonanno, and J. Weiner, *J. Phys. B* **16**, 3015 (1983).

²J. Huennekens and A. Gallagher, *Phys. Rev. A* **28**, 1276 (1983).

³R. Bonanno, J. Boulmer, and J. Weiner, *Phys. Rev. A* **28**, 604 (1983).

⁴V. S. Kushawaha and J. J. Leventhal, *Phys. Rev. A* **25**, 346 (1982).

⁵A. de Jong and F. van der Valk, *J. Phys. B* **12**, L561 (1979).

⁶A. Klucharev, V. Sepman, and V. Vuinovich, *Opt. Spectrosc.* **42**, 366 (1977).

⁷W. D. Phillips and D. E. Pritchard, *Phys. Rev. Lett.* **33**, 1254 (1974).

⁸J. Apt and D. E. Pritchard, *Phys. Rev. Lett.* **37**, 91 (1976).

- ⁹A. Fischer and I. V. Hertel, *Z. Phys. A* **304**, 103 (1982).
- ¹⁰R. Campargue, Ph.D. thesis, Documentation Française, Paris, 1970.
- ¹¹W. H. Miller, *J. Chem. Phys.* **52**, 3563 (1970).
- ¹²C. J. Cerjan, K. K. Docken, and A. Dalgarno, *Chem. Phys. Lett.* **38**, 401 (1976).
- ¹³R. Montagnani, P. Riani, and O. Salvetti, *Chem. Phys. Lett.* **102**, 571 (1983).
- ¹⁴J. G. Kircz, R. Morgenstern, and G. Nienhuis, *Phys. Rev. Lett.* **48**, 610 (1982).
- ¹⁵E. W. Rothe, R. Theyunni, G. P. Reck, and C. C. Tung, *Phys. Rev. A* **31**, 1362 (1985).
- ¹⁶Paul Julienne (private communication).
- ¹⁷F. Masnou-Seeuws *et al.* have sent us preliminary results of new Na(3*p*)-Na(3*p*) potential surface calculations.